applied sciences

MDPI

Article

Effect of Wood Densification and GFRP Reinforcement on the Embedment Strength of Poplar CLT

Akbar Rostampour-Haftkhani [1,*], Farshid Abdoli [2], Mohammad Arabi [3], Vahid Nasir [4,*] and Maria Rashidi [2,*]

[1] Wood Science and Technology, Department of Natural Resources, Faculty of Agriculture and Natural Resources, University of Mohaghegh Ardabili, Ardabil 56199-11367, Iran
[2] Centre for Infrastructure Engineering (CIE), School of Engineering, Design and Built Environment, Western Sydney University, Sydney 2145, Australia; abdolifarshid@gmail.com
[3] Wood Science and Technology, Department of Natural Resources, Faculty of Agriculture and Natural Resources, University of Zabol, Zabol 11936-53471, Iran; marabi@uoz.ac.ir
[4] Department of Wood Science and Engineering, Oregon State University, Corvallis, OR 97331, USA
* Correspondence: arostampour@uma.ac.ir (A.R.-H.); vahid.nasir@oregonstate.edu (V.N.); m.rashidi@westernsydney.edu.au (M.R.)

Abstract: Embedment strength is an important factor in the design and performance of connections in timber structures. This study assesses the embedment strength of lag screws in three-ply cross-laminated timber (CLT) composed of densified poplar wood with densification ratios of 25% and 50%, under both longitudinal (L) and transverse (T) loading conditions. The embedment strength was thereafter compared with that of CLT reinforced with glass-fiber-reinforced polymer (GFRP). The experimental data was compared with results obtained using different models for calculating embedment strength. The findings indicated that the embedment strength of CLT specimens made of densified wood and GFRP was significantly greater than that of control specimens. CLT samples loaded in the L direction showed higher embedment strength compared to those in the T direction. In addition, 50% densification had the best performance, followed by 25% densification and GFRP reinforcement. Modelling using the NDS formula yielded the highest accuracy (mean absolute percentage error = 10.31%), followed by the Ubel and Blub (MAPE = 21%), Kennedy (MAPE = 28.86%), CSA (MAPE = 32.68%), and Dong (MAPE = 40.07%) equations. Overall, densification can be considered as an alternative to GFRP reinforcement in order to increase the embedment strength in CLT.

Keywords: embedment strength; densification; cross-laminated timber

check for updates

Citation: Rostampour-Haftkhani, A.; Abdoli, F.; Arabi, M.; Nasir, V.; Rashidi, M. Effect of Wood Densification and GFRP Reinforcement on the Embedment Strength of Poplar CLT. *Appl. Sci.* **2023**, *13*, 12249. https://doi.org/10.3390/app132212249

Academic Editors: Alena Očkajová, Martin Kučerka and Richard Kminiak

Received: 9 October 2023
Revised: 9 November 2023
Accepted: 10 November 2023
Published: 12 November 2023

1. Introduction

Cross-laminated timber (CLT) is a type of wood product consisting of at least three orthogonal layers of solid-sawn lumber bonded with adhesive, fasteners, or wooden dowels [1]. Timber construction with CLT has gained popularity in both residential and commercial applications.

Due to the load-bearing resistance of CLT, the efficacy of wood structures is highly dependent on the applied connections [2,3]. In CLT structural systems, connections are essential for lateral force transfer and energy dissipation [4]. Carpenter-made mortise and tenon joints are typically found in traditional wood structures, but these conventional connection types are rarely used in contemporary wood structures. Instead, a variety of standard metal connectors and dowels are utilized [5–7]. Various factors can impact the load-bearing capacity of connections between cross-laminated timber (CLT) elements, including the type of wood species and technology used in CLT production, the specific design of the engineering connection, environmental conditions such as ambient temperature and air humidity, the type of applied load (static or dynamic), and the quality of workmanship [8,9].

Connections and fasteners in timber structures are subjected to numerous external loading conditions, including the lateral load. Estimating the embedment strength of CLT is essential, especially under lateral load conditions. In general, embedment strength is a system property representing the resistance of wood to laterally loaded embedment fasteners. When fasteners are inserted into the side face or the narrow face of cross-laminated timber (CLT) at different angles relative to the fastener axis and load, the resulting system property encompasses a range of inputs from the layers and laminations, which is due to the varied load-grain angles [7].

Due to considerable variations in embedment strength, deformation, ductility, and failure modes between the longitudinal and transverse layers, the orthogonal lamination complicates the connection properties of CLT [1]. Additionally, due to the orthogonal lamination, the embedment locations of dowels in CLT become more complicated. It is possible to locate dowels parallel and perpendicular to the grain within and between a single lamina in one layer as well as between layers when dowels are installed on the narrow face of CLT [1]. Similarly, when installed on the flat side of the CLT panel, the dowels may penetrate into multiple layers. Therefore, it is necessary to evaluate the embedment strength in wood structures. The embedment strength of wood is necessary for estimating the capacity of structural timber connectors using dowel-type fasteners. This strength is derived from expressions that are based on tests carried out on timber. Dowel-type connectors are the most frequent form of joint used in modern construction, and they are typically made of wood or metal [10]. Dowel-type connections provide a number of benefits, one of which is their ductile characteristic, which makes it possible for considerable relative deformations and rotations to occur between the wood pieces [11]. Therefore, the embedding strength is not a specific attribute of the material but rather a property of the system. Different empirical equations have been proposed to estimate embedment strength. However, a thorough examination is necessary to develop novel approaches that include relevant derived factors for the designer's benefit [10].

Numerous factors influence the embedment strength of wood and engineered wood products (EWPs), including the type of wood species, density, moisture content, loading direction, dowel diameter, and so on [12].

Multiple studies have evaluated the embedment strength of connectors in CLT. Blaß and Uibel [13] and Uibel and Blaß [14–16] conducted the first investigations of the embedment strength of laterally loaded dowel-type fasteners in CLT. Santos et al. [17] observed that wood density and embedment strength are related. This positive correlation was also reported by [16]. A study on the nail-bearing strength of hybrid CLT composed of Japanese larch and yellow poplar [18] revealed that increasing the higher ratio of minor lamina thickness to nail depth resulted in a lower embedment strength in the hybrid CLT. To obtain effective bearing resistance of the nail connection, the length of the nail used for the mixed CLT should be chosen based on the thickness of the minor lamina. Several additional studies [19–22] have investigated the embedment strength of connectors in CLT and wood-based products. They worked on the embedment strength of EWPs such as CLT made of various wood species.

The timber species used to manufacture CLT significantly affects its properties. Poplar is a fast-growing tree, which is advantageous in nations with a wood supply shortage. Several studies have examined the CLT properties of fast-growing timber species [23–29].

It is essential to reinforce the wood, notably at vulnerable connection points [30]. In addition, the low density of certain wood species, such as poplar, may results in undesirable mechanical properties. There are various techniques to reinforce EWPs and improve the mechanical strength of timber structures, including but not limited to reinforcement using metals or fiber-reinforced polymers (FRPs). According to Saribiyik and Akguuml [31], reinforcing the connections aims to preserve the continuity of structures and lessen the drawbacks of connection elements with nails and bolts. Several investigations on concrete [32,33], metal plates [32,34–36], rods, and bars as reinforcement in wood-based products have been performed.

Additionally, FRPs can be used in different ways for reinforcement [37]. Due to their strength-to-weight ratio, glass-fiber-reinforced polymers (GFRPs) appear to be an optimal fiber type for reinforcing wood components [31]. Douglas fir split timber stringers were strengthened for shear and bending forces with GFRP layers. Depending on the severity of beam fracture prior to reinforcement, the proposed strengthening design increased the stiffness [38]. Hay et al. [39] showed that diagonal (0–90° lay-up) GFRP layers were more effective than vertical ones in shear-strengthening creosote-treated Douglas fir beams with horizontal fractures at their extremities. The mechanical characteristics of connecting points of fiber-reinforced longitudinal notched lap joints fabricated from black pine lumber were investigated [31]. The results demonstrated that GFRP could be utilized as a connecting mechanism for timber members. Wu et al. [40] created a GFRP wood-affixed connection as a replacement due to the potentially corrosive character of steel-plated pine wood connectors. According to their findings, the majority of GFRP wood-bolted connectors failed due to the bearing failure of the bolt openings in the wood panels when subjected to lateral tension load.

Densification is another method for enhancing the mechanical properties of timber and timber-based products that increases the strength, hardness, and abrasion resistance of timber [41]. Densified timber can be utilized by creating laminates and processing the densified wood with a similar construction to that of laminated veneer lumber (LVL), glue-laminated timber (Glulam), and CLT. Feng and Chiang investigated the mechanical strength of CLTs manufactured from densified wood [42]. The use of densified timber enhanced the CLT's bending strength and rigidity, with an increase in modulus of elasticity (MOE) and modulus of rupture (MOR). A similar study on the use of densified wood was conducted by Salca et al. [43], who manufactured and tested densified plywood. MOE, MOR, and shear strength increased, as did the bonding quality of the adhesives between panels.

There is currently a knowledge gap on evaluating the effects of densification and GFRP reinforcement on the embedment strength of CLT manufactured from fast-growing poplar wood. Thus, this study aims to compare the embedment strength of CLT made of densified timber with that of reinforced with GFRP in two loading directions in order to determine which reinforcing technique may be more advantageous. In addition, different approaches are used to calculate the embedment strength and find the model yielding minimum error compared to the experimental data.

2. Materials and Methods

2.1. Materials and CLT Fabrication

Three-ply CLT panels made of air-dried poplar (*Populus alba*) wood with moisture content of around 12% and oven-dry density of 400 ± 10 kg/m^3 were used in this research. CLT panels were produced in four groups. The thickness of the boards was 2 cm. One group was reinforced with GFRP using a bidirectional (0°/90°) E-glass fiber fabric (fiber tensile modulus and density of 70 GPa and 2.55 gr/cm^3, respectively), as shown in Figure 1. Three GFRP layers were added to each surface. Two groups were manufactured with densified wood in two densification ratios (25% and 50%). In order to manufacture densified wood, lumber panels were placed between heated platens in a hydraulic press and compressed. Then, CLT panels were made from the densified wood. The last group consisted of CLT with non-densified wood, considered as a control group (0). A summary of the sample groups is detailed in Table 1. All components were cold-pressed for 150 min and pressure of 1 MPa with one-component polyurethane glue.

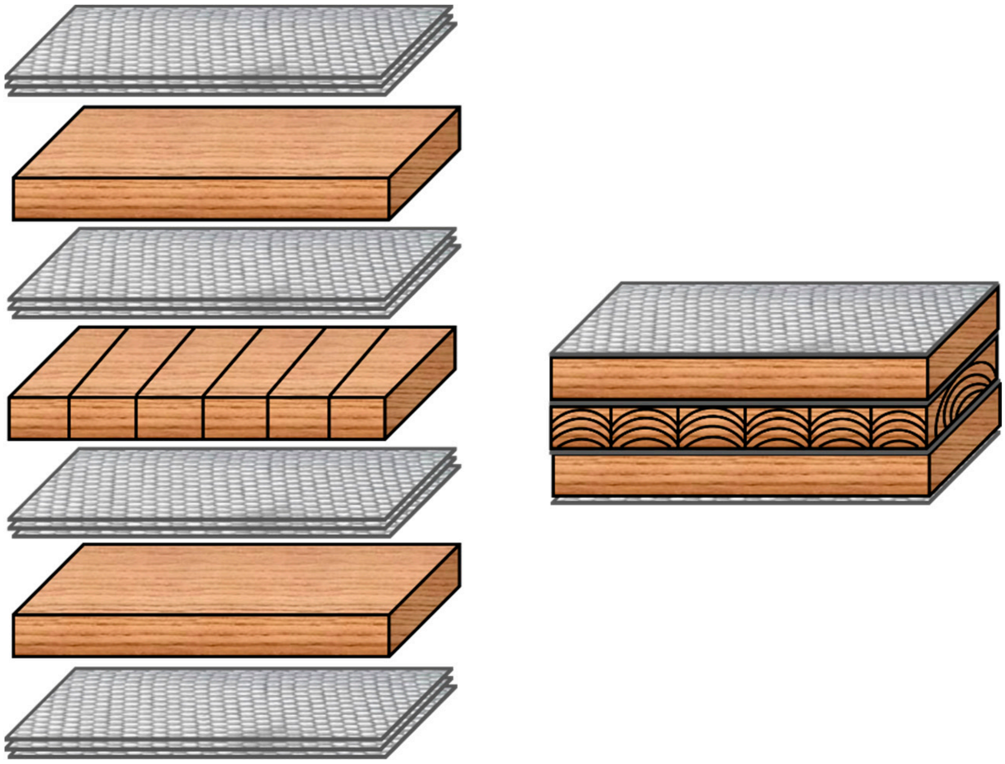

Figure 1. GFRP arrangement in CLT layers.

Table 1. Sample groups and repetitions.

Sample Groups	Repetitions	Description
Control (unreinforced) 0L, 0T	10	No reinforcement (Loading direction: L = longitudinal, T = transverse)
25L	10	Reinforcement with 25% densification (loading direction: longitudinal)
25T	10	Reinforcement with 25% densification (loading direction: transverse)
50L	10	Reinforcement with 50% densification (loading direction: longitudinal)
50T	10	Reinforcement with 50% densification (loading direction: transverse)
GFRPL	10	Reinforcement with GFRP (loading direction: longitudinal)
GFRPT	10	Reinforcement with GFRP (loading direction: transverse)

Embedment Strength Modelling and Experiments

After preparing the CLT panel, specimens with dimensions of 15 cm × 8 × cm × 6 cm (length × width × thickness) were cut from the panel for the embedment strength test (Figure 2). A lag screw (s) with a diameter of 8 mm was used as a fastener. The characteristics of the fastener are detailed in Table 2.

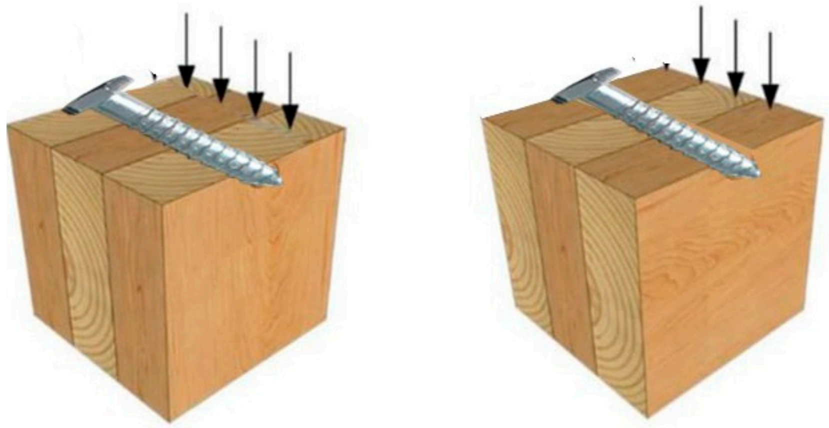

(**a**) (**b**)

Figure 2. Loading directions of CLT samples for embedment strength: (**a**) loading in longitudinal (L) direction; (**b**) loading in transverse (T) direction.

Table 2. Characteristics of lag screw.

Lag Screw (DIN 571)	Length of the Screw (L) (mm)	Head Height (K) (mm)	Da (mm)	Ds (mm)	Length of the Thread (b) (mm)
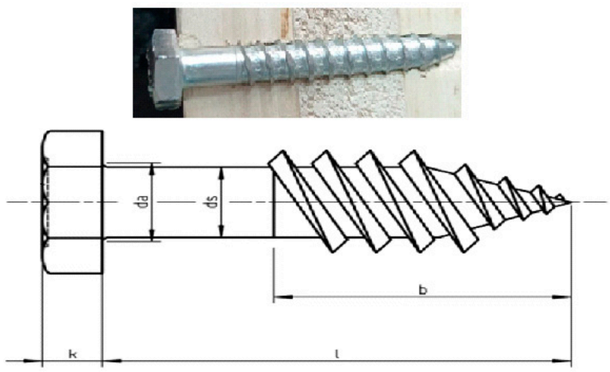	54	5.5	8.5	7	44

Finally, the embedment strength (σ) was calculated using $\sigma\left(\frac{\mathrm{N}}{\mathrm{mm}^2}\right) = \frac{F}{\mathrm{A}}$, in which *F* is the yield load obtained from the 5% offset method (N) and A is the embedment area (mm^2).

To determine the embedment strength, specimens were subjected to loading in two directions of longitudinal (L) and transverse (T), as shown in Figure 3 using a Hounsfield testing equipment model 0308 (Figure 3) and a loading pace of 5 mm/min.

Figure 3. The loading apparatus of CLT samples for embedment strength testing.

2.2. Statistical Analysis

The data was assessed statistically as a complete factorial design consisting of two factors using the SPSS 25 program. The densification ratio (in three levels: 0, 25, and 50) and two CLT loading directions (L and T directions) were the two factors that were taken into consideration for the statistical analysis. ANOVA test used to analyze those factors statistically through the main and interaction effects. Afterward, the results (means) of densified CLT samples were compared to those reinforced with GFRP. Four different sample groups, each with ten replicates, were put through their paces throughout the testing process. These sample groups included control (unreinforced) CLT specimens, CLT samples with 25% densified layers, CLT samples with 50% densified layers, and CLT samples reinforced with GFRP, all of which were loaded in both the longitudinal (L) and transverse (T) directions. The statistical differences between the means were analyzed using the multiple range test developed by Duncan with a confidence level of 95%.

2.3. Embedment Strength Equations

Currently, a number of distinct models of computation for CLT embedment strength are available. The most important calculation models are discussed in this part so that a comparison can be made between them.

The Kennedy [44], NDS [45], Ubel and Blub [46], Dong [2], and CSA [47] equations were used in this study to predict the embedment strength of CLT. These equations were developed based on various factors, such as density, loading direction, and so on.

Kennedy et al. conducted a comprehensive study including about 720 embedment tests on Canadian cross-laminated timber (CLT) using lag screws, as well as 360 tests using self-drilling screws. The experiments included a range of screw sizes from 6.0 mm to 19.1 mm. A regression model that is not influenced by the panel layup and fastener diameter was constructed. According to Kennedy's model, the embedment strength is calculated as follows:

$$f_{\theta,avg,Ken} = \frac{80(\rho_{12} - 0.12)^{1.11}}{1.07(\rho_{12} - 0.12)^{-0.07} sin^2\theta + cos^2\theta} \quad (1)$$

where $f_{\theta,avg}$ is average embedment strength (MPa), ρ_{12} is density at 12% moisture content (g/cm^3), and θ is loading angle relative to the grain of face layer (°).

Based on the NDS model, the strength of the face layer's embedment is linked to the "effective" bearing length of the fastener. This bearing length is changed proportionally based on the embedment strengths of both the transverse layer and the longitudinal layer.

According to the NDS model, the embedment strength is calculated as follows:

$$f_{\theta,avg,NDS} = \frac{\ell_{\parallel}}{\ell_{\rho}} . \frac{77G_0}{0.36{G_0}^{-0.45} d^{0.5} sin^2\theta + cos^2\theta} + \frac{\ell_{\perp}}{\ell_{\rho}} . \frac{77G_0}{0.36{G_0}^{-0.45} d^{0.5} cos^2\theta + sin^2\theta} \quad (2)$$

where G_0 is measured relative density for the species or species group based on oven-dry mass and volume; $\ell_{\parallel}$ is the lag screw embedment length in parallel layer (s); $\ell_{\perp}$ is the lag screw embedment length in cross layer (s); ℓ_{ρ} is the embedment length of the lag screw in CLT specimen; and d is fastener diameter (mm).

Ubel and Blub conducted pioneering research on the lateral loading behavior of dowel-type fasteners in cross-laminated timber (CLT) panels. The researchers conducted experiments on smooth dowels ranging in diameter from 8 mm to 24 mm. These dowels were tested in both three- and five-layer cross-laminated timber (CLT) components. The dowels were strategically placed at gaps of one to three layers and subjected to loading at angles of 0°, 45°, and 90° with respect to the grain orientation of the face layer. The model is formulated as a mathematical expression that incorporates the variables of fastener diameter, overall wood density of the panel, and loading direction in relation to the strength axis of the panel, namely the grain direction of the surface layers of the cross-laminated timber (CLT) panel.

According to Ubel and Blub's model, the embedment strength is calculated as follows:

$$f_{\theta,avg,UB} = 111.7(1 - 0.016d)\,\rho_{12}^{1.16} \times \left[\frac{\sum_{i=1}^{n} t_{0,i}}{t\left(1.2sin^2\theta + cos^2\theta\right)} + \frac{\sum_{j=1}^{n-1} t_{90,j}}{t\left(1.2cos^2\theta + sin^2\theta\right)} \right] \quad (3)$$

where $t_{0,i}$ is the thickness of the CLT longitudinal layer i, and $t_{90,j}$ the thickness of the CLT transverse layer i.

According to Dong's model, the embedment strength is calculated as follows:

$$f_{\theta,avg,Dong} = 336.4(0.45 - 0.02d)\,\rho_{12} \times \left(\frac{R_t}{1.41cos^2\theta + sin^2\theta} + \frac{1 - R_t}{1.41sin^2\theta + cos^2\theta}\right) \quad (4)$$

where R_t the ratio between the total thickness of the transverse layers and the CLT thickness.

According to the CSA's model, the embedment strength is calculated as follows:

$$f_{\theta,avg,CSA} = \frac{0.9 \times 82_{\rho_{12}}(1 - 0.01d)}{0.9 \times 2.27sin^2\theta + cos^2\theta} \quad (5)$$

All of the notation used in all equations is mentioned above. Mean absolute percentage error (MAPE) values were used to evaluate the prediction performance of each model as follows (Equation (6)):

$$MAPE = \frac{1}{n}\sum_{i=1}^{n}\left(\frac{|y_i - y_p|}{y_i}\right)100 \quad (6)$$

where y_i is the experimental value, y_p is the predicted value, and n is the total amount of data. The lower the MAPE values, the smaller the difference between experimental and predicted values.

3. Results and Discussion

Effect of Densification Ratio and Loading Direction on Embedment Strength

With a confidence level of 95% (p-value > 0.05), the results of the analysis of variance (ANOVA) shown in Table 3 suggest that both the densification ratio and the loading direction had significant main impacts on embedment strength.

Table 3. ANOVA table for main and interaction effects of densification ratio and loading direction on embedment strength of CLT samples.

Property	Source	df	Mean Square	F	Sig.
Embedment strength	Densification ratio	2	2079.221	124.640	0.000 **
	Loading direction	1	151.877	9.104	0.004 **
	Densification ratio × loading direction	2	4.520	0.271	0.764 ns

** significant at 99% confidence level, ns non-significant.

As can be seen in Table 4, when compared to the control specimens, the embedment strength of CLT samples improved by 46% and 66.8%, respectively, with a 25% and 50% increase in densification ratio. Furthermore, it was discovered that the embedment strength of the CLT samples was 8% greater in the longitudinal (L) direction compared to the transverse (T) direction when the main effect of the loading direction of the CLT samples on embedment strength was considered. This was due to the fact that both of these factors were changed simultaneously. In addition, the findings showed that the embedment strength of CLT samples with a densification ratio of 0 (control samples), 25%, and 50% in the longitudinal loading direction of CLT samples was 10.9%, 5.4%, and 8.8% greater, respectively, compared to the transverse loading direction.

Table 4. Main and interaction effects of densification ratio and loading direction on embedment strength of CLT samples with Duncan test results.

Main Effects			
Densification ratio	0	29.8 (4.65) *	A **
	25	43.7 (3.4)	B
	50	49.7 (4.76)	C
Loading direction	T	39.44 (9.29)	A
	L	42.62 (9.41)	B
Interaction effects			
Densification ratio	**Loading direction**	**Embedment strength (MPa)**	
0	T	28.24 (4.88)	A
	L	31.33 (4.07)	A
25	T	42.52 (3.61)	B
	L	44.8 (2.92)	BC
50	T	47.58 (4.19)	C
	L	51.75 (4.54)	D

* The values in parentheses represent standard deviation. ** The letters show Duncan test results.

Comparing the embedment strength of CLT samples manufactured from densified wood and those reinforced with GFRP was one of the goals of this investigation. The embedment strength of the GFRP-reinforced CLT samples was compared with that of CLT samples constructed out of densified wood, and the average embedment strength of the CLT specimens is illustrated in Figure 4. The highest embedment strength belonged to the 50L samples (51.75 MPa), while the lowest embedment strength belonged to the 0T samples (28.24 MPa). The embedment strength of the CLT samples in the L direction was greater than in the T direction. More specifically, the embedment strength of 0L, 25L, 50L, and GFRPL samples was 10.9%, 5.4%, 8.8%, and 6.8% more, respectively, than that of their counterpart samples tested in transverse direction. Reinforcement with 25% densification, 50% densification, and GFRP improved the embedment strength by 43%, 65.2%, and 43.4%, respectively, compared to the unreinforced samples in the L direction (0L). On the other hand, reinforcement with 25% densification, 50% densification, and GFRP improved the embedment strength by 50.6%, 68.5%, and 49%, respectively, compared to the unreinforced samples in the T direction (0T). In addition, no significant difference was observed in the embedment strength of reinforced CLT samples with 25% densification and GFRP in both directions (L and T). Therefore, it can be concluded that CLT with the same embedment strength can be produced using wood with a densification ratio of 25% rather than reinforcing it with GFRP. This alternate method demonstrates more efficiency in terms of both its cost and implementation. Previously, it was reported that embedment strength perpendicular to the grain was lower than that parallel to the grain [1,2,48,49]. Reinforcement with densification enhanced the wood density resulting in higher embedment strength of CLT samples. From a designer's point of view, wood density and dowel diameter are the main properties of design. There are also some approaches where density is the only parameter [22,50]. Concerning face side insertion in CLT, Uibel and Blab [15,46] evaluated the load-bearing capacity of dowels placed in manufactured with four distinct arrangements and computed the embedment strength. The CLT embedment strength prediction model was suggested based on the variable CLT lamination characteristics.

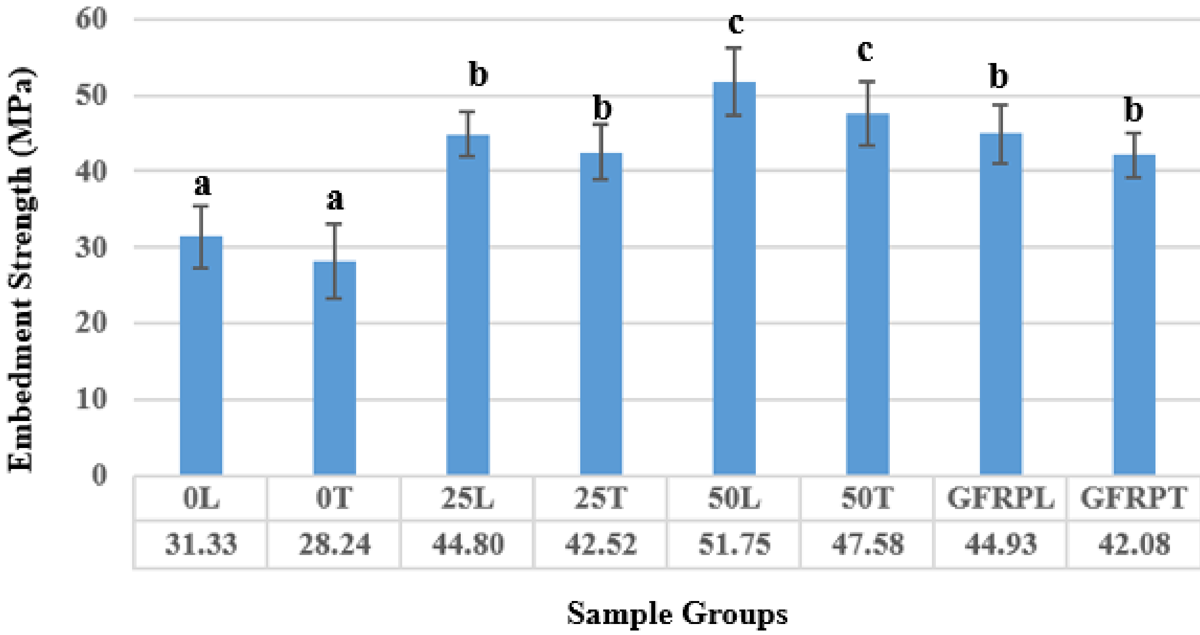

Figure 4. Means and standard deviations of embedment strength of control, densified, and GFRP-reinforced CLT specimens.

The load displacement of control, densified, and GFRP-reinforced CLT specimens is shown are Figure 5. Accordingly, the yield points of the CLT samples in the L direction were more than those in T direction. The yield points of 0L, 25L, 50L, and GFRPL were 8636 (N), 11,900 (N), 16,080 (N), and 13,720 (N), respectively. The highest yield point in the L direction belonged to the CLT sample reinforced with 50% densified wood. On the other hand, the yield points of 0T, 25T, 50T, and GFRPT were 7947 (N), 11,450 (N), 13,152 (N), and 12,120 (N), respectively. The highest yield point in the L direction belonged to the CLT sample reinforced with 50% densified wood.

The failure modes of CLT specimens are depicted in Figure 6. The typical failure modes of tested CLT specimens are different in the situation where the lag screw is loaded in the L and T direction of the CLT specimens. Cracks occurred along the grain when the load was applied along with the L direction, as shown in Figure 6 (0L, 25L, and 50L). Cracks in 25L and 50L show that the densification reduced the length of the cracks compared to the unreinforced samples (0L). However, compression failure occurred in the embedment surface, as shown in Figure 6 (0T, 25T, 50T, GFRPL, and GFRPT), or cracks appeared on both edges of the cross layers, as shown in Figure 6 (0T), when the CLTs were loaded in the T direction. The compression failure might occur layer by layer, which results in stress redistribution [1].

The results of the prediction models in comparison with experimental results are shown in Figure 7. NDS showed the most accurate results compared to the experimental findings, followed by the Ubel and Blub and then the Kennedy and CSA formulas. Finally, the formula of Dong et al. showed the lowest accuracy in terms of the prediction of experimental results. Previously, all of these equations were applied to predict the embedment strength of fasteners in EWPs, such as CLT. Accordingly, various results were obtained regarding the accuracy of these equations. The accuracy of the equations might be related to factors including moisture content, density, diameter of fastener, or the loading direction.

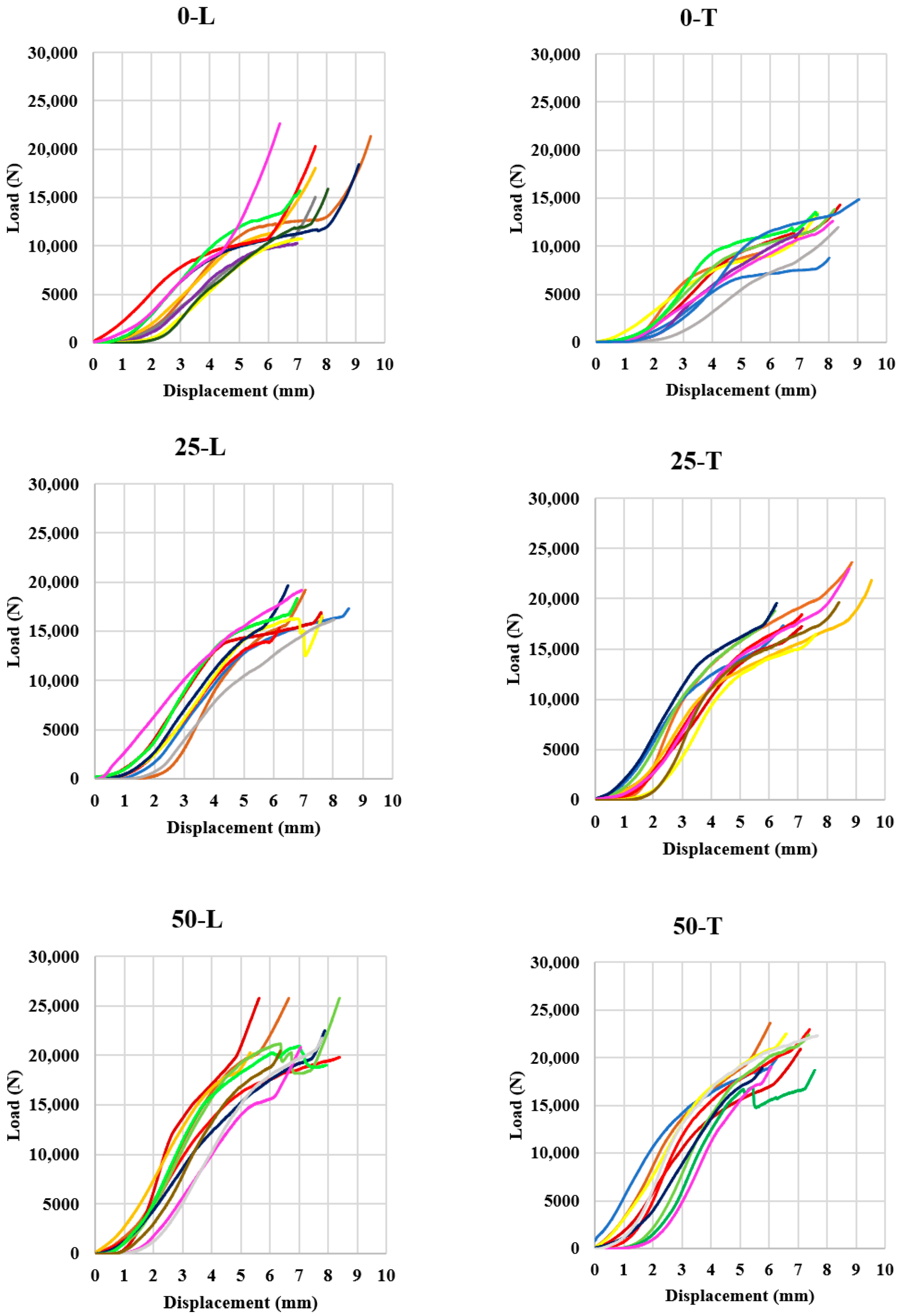

Figure 5. *Cont.*

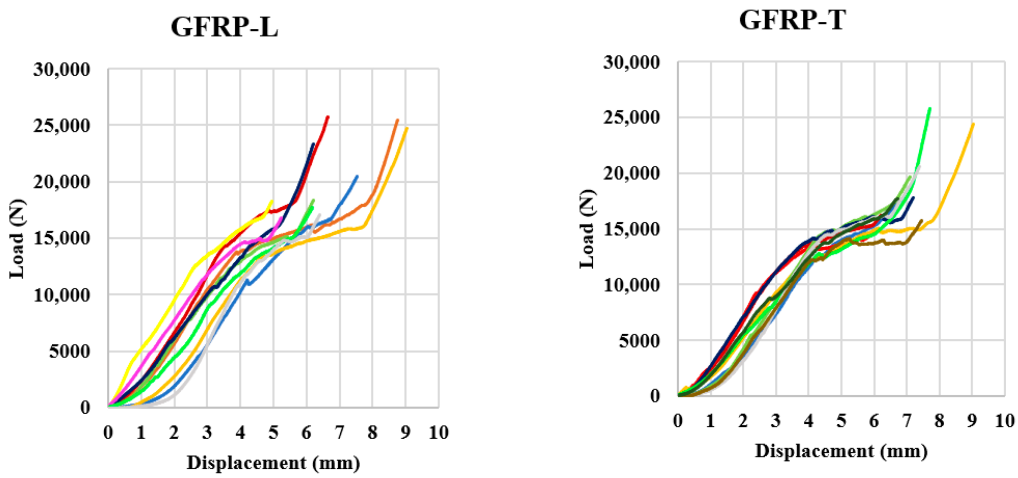

Figure 5. Load-displacement curves of the reinforced and unreinforced CLT samples.

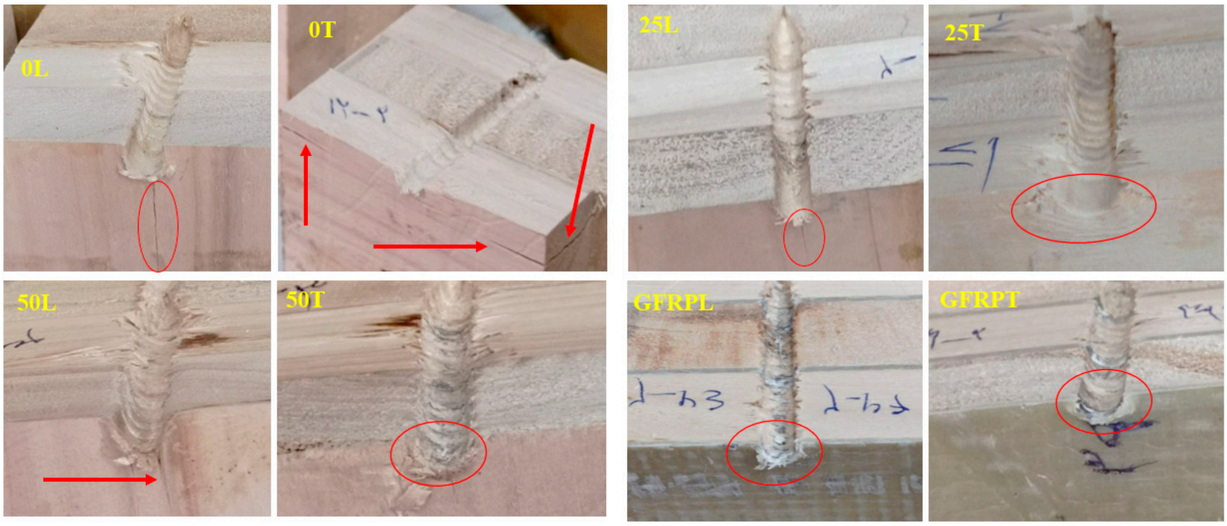

Figure 6. Failure modes of reinforced and unreinforced CLT specimens in L and T loading directions.

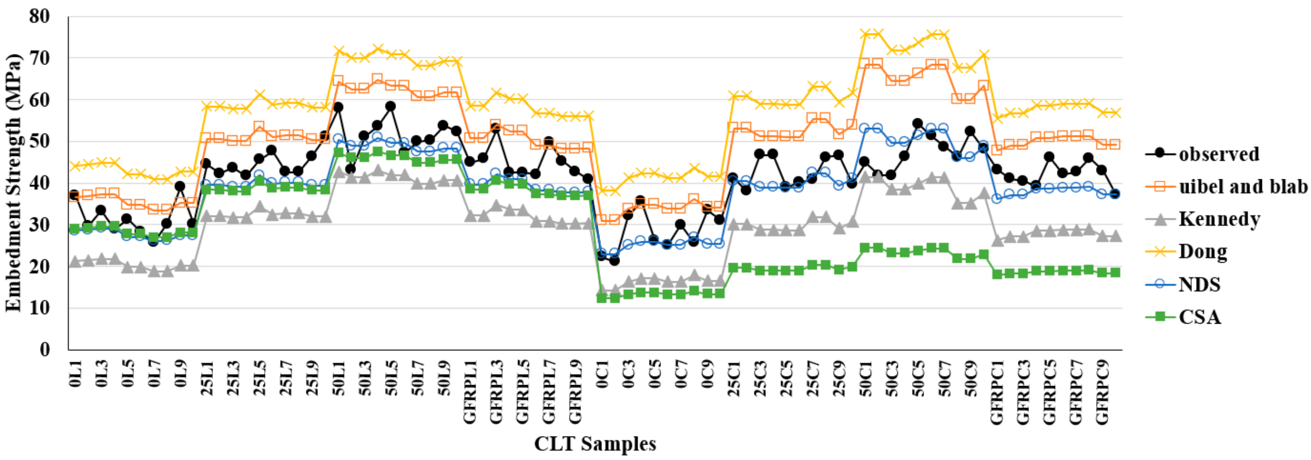

Figure 7. Comparison of the observed and predicted values of the embedment strength.

The MAPE of all models is detailed in Table 5. The NDS formula showed the highest accuracy (10.31%). After that, the Ubel and Blub formula showed the highest accuracy (21.3%). On the other hand, Dong et al.'s formula showed the lowest accuracy (40.07%). These findings indicate that the NDS and Ubel and Blub formulas are reliable in predicting embedment strength in the tests related to loading directions and reinforcement factors. The MAPE classification approach, which was established by Lewis [51], was used in this investigation for the purpose of determining how accurately prediction models performed. This categorization assigns models into one of four accuracy categories based on their mean absolute percentage error (MAPE): excellent (MAPE < 10%), acceptable (MAPE 10–19%), fair (MAPE 20–49%), and weak (MAPE $\geq$ 50%). Future studies could consider developing machine learning modeling for embedment strength prediction. In addition, nondestructive testing methods such as acoustic emission monitoring could be used to further investigate the failure mechanism [52].

Table 5. MAPE of equations for predicting embedment strength of CLT specimens.

MAPE (%)				
Ubel and Blab	Kennedy	Dong et al.	NDS	CSA
21.30	28.86	40.07	10.31	32.68

4. Conclusions

This work evaluated the embedment strength of 3-ply poplar CLT samples reinforced with GFRP and densified wood (25% and 50%) in two loading directions (L and T). Overall, reinforcement improved the embedment strength of CLT samples. The embedment strength of CLT samples in the L loading direction (outer layers to the same fiber direction) was greater than those in the T loading direction. CLT samples made from 50% densified poplar wood showed the highest embedment strength (50L: 51.75 MPa and 50T: 47.58 MPa). However, there was no significant difference in embedment strength between CLT samples reinforced with GFRP and CLT samples made from 25% densified wood (25L: 44.8 MPa, GFRPL: 44.93 MPa, 25T: 42.52 MPa, and GFRPT: 42.08 MPa). Modelling using the NDS formula yielded the highest accuracy (MAPE = 10.31%), followed by the Ubel and Blub (MAPE = 21%), Kennedy (MAPE = 28.86%), CSA (MAPE = 32.68%), and Dong (MAPE = 40.07%) equations. Densification can be considered as an alternative to GFRP reinforcement in order to increase the embedment strength in CLT. Statistical analysis showed that in terms of main effects, densification ratio and loading direction significantly affect the embedment strength. However, in terms of interaction effects, both densification ratio and loading direction at the same time had no significant effect on the embedment strength.

Further studies are recommended to evaluate the embedment strength of CLT reinforced with GFRP and densified wood made of more than three layers. Further studies are recommended to evaluate the embedment strength of various types of nails and screws in CLT reinforced with GFRP and densified wood. According to the results of this study, considering the cost of the products, 25% densification might be used instead of GFRP for CLT reinforcement. However, further investigations regarding the effects of densification on CLT properties, such as bending, glue line, and debonding, are required.

Author Contributions: Conceptualization, A.R.-H. and M.A.; methodology, A.R.-H. and M.A.; formal analysis, A.R.-H., F.A. and M.A.; resources, A.R.-H., F.A. and M.A.; writing—original draft preparation, F.A.; writing—review and editing, A.R.-H., V.N. and F.A.; visualization, F.A., supervision, A.R.-H. and M.R.; project administration, A.R.-H., V.N. and M.R. All authors have read and agreed to the published version of the manuscript.

Funding: This research received no external funding.

Institutional Review Board Statement: Not applicable.

Informed Consent Statement: Not applicable.

Data Availability Statement: The data is not publicly available as it is part of some ongoing research by the authors. However, they may be available upon reasonable request from corresponding authors.

Conflicts of Interest: The authors declare no conflict of interest.

References

1. Dong, W.; Li, Q.; Wang, Z.; Zhang, H.; Lu, X.; Gong, M. Effects of embedment side and loading direction on embedment strength of cross-laminated timber for smooth dowels. *Eur. J. Wood Wood Prod.* **2020**, *78*, 17–25. [CrossRef]
2. Dong, W.; Wang, Z.; Zhou, J.; Zhang, H.; Yao, Y.; Zheng, W.; Gong, M.; Shi, X. Embedment strength of smooth dowel-type fasteners in cross-laminated timber. *Constr. Build. Mater.* **2020**, *233*, 117243. [CrossRef]
3. Rashidi, M.; Hoshyar, A.N.; Smith, L.; Samali, B.; Siddique, R. A comprehensive taxonomy for structure and material deficiencies, preventions and remedies of timber bridges. *J. Build. Eng.* **2021**, *34*, 101624. [CrossRef]
4. Bora, S.; Sinha, A.; Barbosa, A.R. Effect of Short-Term Simulated Rain Exposure on the Performance of Cross-Laminated Timber Angle Bracket Connections. *J. Archit. Eng.* **2022**, *28*, 04022025. [CrossRef]
5. Ling, T.; Mohrmann, S.; Li, H.; Bao, N.; Gaff, M.; Lorenzo, R. Review on research progress of metal-plate-connected wood joints. *J. Build. Eng.* **2022**, 105056. [CrossRef]
6. Ringhofer, A.; Brandner, R.; Blaß, H.J. Cross laminated timber (CLT): Design approaches for dowel-type fasteners and connections. *Eng. Struct.* **2018**, *171*, 849–861. [CrossRef]
7. Ling, Z.; Rong, X.; Xiang, Z. Laterally loaded performance of single dowel-type fastener used for steel plate-to-timber connections. In *Structures*; Elsevier: Amsterdam, The Netherlands, 2021; pp. 1985–1997.
8. Sydor, M.; Rogoziński, T.; Stuper-Szablewska, K.M.; Starczewski, K. The accuracy of holes drilled in the side surface of plywood. *BioResources* **2020**, *15*, 117–129. [CrossRef]
9. Sydor, M.; Majka, J.; Rychlik, M.; Turbański, W. Application of 3D Scanning Method to Assess Mounting Holes' Shape Instability of Pinewood. *Materials* **2023**, *16*, 2053. [CrossRef]
10. Yurrita, M.; Cabrero, J.M. New criteria for the determination of the parallel-to-grain embedment strength of wood. *Constr. Build. Mater.* **2018**, *173*, 238–250. [CrossRef]
11. Jorissen, A.; Fragiacomo, M. General notes on ductility in timber structures. *Eng. Struct.* **2011**, *33*, 2987–2997. [CrossRef]
12. Zhang, X.; Yin, H.; Zhao, E.; Li, S.; Liu, Q. Experimental investigation on embedment strength of bamboo-based composite prepared with the inorganic adhesive. *J. Build. Eng.* **2023**, *76*, 107323. [CrossRef]
13. Blaß, H.J.; Uibel, T. *Tragfähigkeit von Stiftförmigen Verbindungsmitteln in Brettsperrholz*; Karlsruher Institut für Technologie: Karlsruhe, Germany, 2007.
14. Uibel, T.; Blaß, H.J. Edge joints with dowel type fasteners in cross laminated timber. In Proceedings of the CIB-W18 Meeting, Bled, Slovenia, 8 August 2007.
15. Uibel, T.; Blaß, H.J. Joints with dowel type fasteners in CLT structures. In Proceedings of the Focus Solid Timber Solutions-European Conference on Cross Laminated Timber (CLT), Bath, UK, 21–22 May 2013; pp. 119–136.
16. HJ, B. Load-carrying capacity of joints with dowel-type fasteners and interlayers. In Proceedings of the CIB-W18, Delft, 2000, Florence, Italy, 16–19 August 2000.
17. Santos, C.; De Jesus, A.; Morais, J.; Lousada, J. A comparison between the EN 383 and ASTM D5764 test methods for dowel-bearing strength assessment of wood: Experimental and numerical investigations. *Strain* **2010**, *46*, 159–174. [CrossRef]
18. Kim, K. Predicting Nail Withdrawal Resistance and Bearing Strength of Cross-laminated Timbers from Mixed Species. *BioResources* **2021**, *16*, 4027–4038. [CrossRef]
19. Ottenhaus, L.-M.; Li, M.; Smith, T. Analytical derivation and experimental verification of overstrength factors of dowel-type timber connections for capacity design. *J. Earthq. Eng.* **2022**, *26*, 2970–2984. [CrossRef]
20. Ou, J.; Yang, X.; Xu, Q. Experimental research on the embedment strength of cross-laminated timber. *Sichuan Build. Sci.* **2020**, *46*, 28–35.
21. Hongyuan, T.; Menglin, M.; Yuan, Y.; Ruizhong, L.; Zhaoyang, Y. Experimental study on dowel bearing strength of cross-laminated-timber (CLT) panels. *J. Build. Struct.* **2022**, *43*, 175.
22. Sandhaas, C.; Ravenshorst, G.; Blass, H.; Van de Kuilen, J. Embedment tests parallel-to-grain and ductility aspects using various wood species. *Eur. J. Wood Wood Prod.* **2013**, *71*, 599–608. [CrossRef]
23. Abdoli, F.; Rashidi, M.; Rostampour-Haftkhani, A.; Layeghi, M.; Ebrahimi, G. Withdrawal performance of nails and screws in cross-laminated timber (CLT) made of Poplar (*Populus alba*) and Fir (*Abies alba*). *Polymers* **2022**, *14*, 3129. [CrossRef]
24. Abdoli, F.; Rashidi, M.; Rostampour-Haftkhani, A.; Layeghi, M.; Ebrahimi, G. Effects of fastener type, end distance, layer arrangement, and panel strength direction on lateral resistance of single shear lap joints in cross-laminated timber (CLT). *Case Stud. Constr. Mater.* **2023**, *18*, e01727. [CrossRef]
25. Rostampour Haftkhani, A.; Rashidi, M.; Abdoli, F.; Gerami, M. The effect of GFRP wrapping on lateral performance of double shear lap joints in cross-laminated timber as a part of timber bridges. *Buildings* **2022**, *12*, 1678. [CrossRef]
26. Kramer, A.; Barbosa, A.R.; Sinha, A. Viability of hybrid poplar in ANSI approved cross-laminated timber applications. *J. Mater. Civ. Eng.* **2014**, *26*, 06014009. [CrossRef]

27. Wang, Z.; Fu, H.; Chui, Y.-H.; Gong, M. Feasibility of using poplar as cross layer to fabricate cross-laminated timber. In Proceedings of the World Conference on Timber Engineering, Quebec City, QC, Canada, 10–14 August 2014.
28. Hematabadi, H.; Madhoushi, M.; Khazaeian, A.; Ebrahimi, G. Structural performance of hybrid Poplar-Beech cross-laminated-timber (CLT). *J. Build. Eng.* **2021**, *44*, 102959. [CrossRef]
29. Hematabadi, H.; Madhoushi, M.; Khazaeyan, A.; Ebrahimi, G.; Hindman, D.; Loferski, J. Bending and shear properties of cross-laminated timber panels made of poplar (*Populus alba*). *Constr. Build. Mater.* **2020**, *265*, 120326. [CrossRef]
30. Lukaszewska, E.; Fragiacomo, M.; Johnsson, H. Laboratory tests and numerical analyses of prefabricated timber-concrete composite floors. *J. Struct. Eng.* **2010**, *136*, 46–55. [CrossRef]
31. Saribiyik, M.; Akgül, T. GFRP bar element to strengthen timber connection systems. *Sci. Res. Essays* **2010**, *5*, 1713–1719.
32. Miotto, J.L.; Dias, A.A. Evaluation of perforated steel plates as connection in glulam–concrete composite structures. *Constr. Build. Mater.* **2012**, *28*, 216–223. [CrossRef]
33. Nie, Y.; Valipour, H. Experimental and numerical study of long-term behaviour of timber-timber composite (TTC) connections. *Constr. Build. Mater.* **2021**, *304*, 124672. [CrossRef]
34. Clouston, P.; Bathon, L.A.; Schreyer, A. Shear and bending performance of a novel wood–concrete composite system. *J. Struct. Eng.* **2005**, *131*, 1404–1412. [CrossRef]
35. Otero-Chans, D.; Estévez-Cimadevila, J.; Suárez-Riestra, F.; Martín-Gutiérrez, E. Experimental analysis of glued-in steel plates used as shear connectors in Timber-Concrete-Composites. *Eng. Struct.* **2018**, *170*, 1–10. [CrossRef]
36. Chybiński, M.; Polus, Ł. Mechanical behaviour of aluminium-timber composite connections with screws and toothed plates. *Materials* **2021**, *15*, 68. [CrossRef]
37. Raftery, G.M.; Whelan, C. Low-grade glued laminated timber beams reinforced using improved arrangements of bonded-in GFRP rods. *Constr. Build. Mater.* **2014**, *52*, 209–220. [CrossRef]
38. Gómez, S.; Svecova, D. Behavior of split timber stringers reinforced with external GFRP sheets. *J. Compos. Constr.* **2008**, *12*, 202–211. [CrossRef]
39. Hay, S.; Thiessen, K.; Svecova, D.; Bakht, B. Effectiveness of GFRP sheets for shear strengthening of timber. *J. Compos. Constr.* **2006**, *10*, 483–491. [CrossRef]
40. Wu, C.; Zhang, Z.; Tam, L.-h.; Feng, P.; He, L. Group effect of GFRP-timber bolted connections in tension. *Compos. Struct.* **2021**, *262*, 113637. [CrossRef]
41. Cabral, J.P.; Kafle, B.; Subhani, M.; Reiner, J.; Ashraf, M. Densification of timber: A review on the process, material properties, and application. *J. Wood Sci.* **2022**, *68*, 20. [CrossRef]
42. Feng, T.Y.; Chiang, L.K. Effects of densification on low-density plantation species for cross-laminated timber. In Proceedings of the AIP Conference Proceedings, Kuala Lumpur, Malaysia, 26–28 August 2019.
43. Salca, E.-A.; Bekhta, P.; Seblii, Y. The effect of veneer densification temperature and wood species on the plywood properties made from alternate layers of densified and non-densified veneers. *Forests* **2020**, *11*, 700. [CrossRef]
44. Kennedy, S.; Salenikovich, A.; Munoz, W.; Mohammad, M. Design equations for dowel embedment strength and withdrawal resistance for threaded fasteners in CLT. In Proceedings of the World Conference on Timber Engineering, Quebec, QC, Canada, 10–14 August 2014; pp. 10–14.
45. National Design Specification (NDS). *National Design Specification (NDS) for Wood Construction–with Commentary*, 2015th ed.; American Wood Council: Leesburg, VA, USA, 2014.
46. Uibel, T.; Blaß, H.J. Load carrying capacity of joints with dowel type fasteners in solid wood panels. In Proceedings of the CIB-W18 Meeting, Bled, Slovenia, 8 August 2007.
47. *CSA. O86-14*; Engineering Design in Wood. Canadian Standards Association: Mississauga, ON, Canada, 2014.
48. Long, W.; Ou, J.; Sun, X.; Huang, X.; He, M.; Li, Z. Experimental study on the embedment strength of smooth dowels inserted in cross-laminated timber narrow side. *J. Wood Sci.* **2022**, *68*, 1–18. [CrossRef]
49. Tuhkanen, E.; Mölder, J.; Schickhofer, G. Influence of number of layers on embedment strength of dowel-type connections for glulam and cross-laminated timber. *Eng. Struct.* **2018**, *176*, 361–368. [CrossRef]
50. Sawata, K.; Yasumura, M. Determination of embedding strength of wood for dowel-type fasteners. *J. Wood Sci.* **2002**, *48*, 138–146. [CrossRef]
51. Lewis, C.D. *Industrial And Business Forecasting Methods: A Practical Guide to Exponential Smoothing and Curve Fitting*; Butterworth Scientific: Oxford, UK, 1982.
52. Nasir, V.; Ayanleye, S.; Kazemirad, S.; Sassani, F.; Adamopoulos, S. Acoustic emission monitoring of wood materials and timber structures: A critical review. *Constr. Build. Mater.* **2022**, *350*, 128877. [CrossRef]